Power Factor Enhancement of Induction Machines by Means of Solid-State Excitation

EDUARD MULJADI, MEMBER, IEEE, THOMAS A. LIPO, FELLOW, IEEE, AND DONALD W. NOVOTNY, FELLOW, IEEE

Abstract—**A new concept for power factor correction of induction machines is introduced that employs an auxiliary three-phase stator winding together with a pulsewidth modulated (PWM) inverter to supply excitation power to the machine. When the PWM inverter is modelled as an equivalent capacitor, it is shown that two values of capacitance will yield unity power factor at a given operation condition. The effect of machine parameters on the critical value of capacitance is examined. A control algorithm to ensure unity power factor at the terminals of the main stator windings is presented and its satisfactory operation verified by means of a detailed analog computer simulation.**

INTRODUCTION

ONE major drawback of an induction machine compared to synchronous machines is its lack of flexibility in the choice of power factor. While the reactive power required by a synchronous machine can be taken from the power source or supplied by the machine itself by adjustment of the field current, the power factor of an induction machine is always lagging and set by external quantities (i.e., the load and terminal voltage). Poor power factor adversely affects the economics of the transmission and distribution system and a cost penalty is frequently levied for excessive var consumption. Power factor is typically improved by installation of capacitor banks, but these banks can cause problems at light load conditions or during loss of supply. Comparatively expensive switchgear is required to vary the capacitance value as the load changes and to disconnect the bank during loss of supply.

The problems involved with discrete switching of capacitors can be greatly overcome by use of solid-state reactive power compensators. A variety of reactive power compensators has been developed to provide power factor correction [1]–[6]. However, these compensators are typically also harmonic generators and require additional capacitors and inductors to provide filtering for the harmonics introduced by the solid-state compensator itself.

In this paper a new configuration employing a combination of a special purpose induction machine and a PWM voltage inverter is proposed. In particular, the machine is equipped with two electrically isolated but magnetically coupled three-phase windings. One three-phase winding set (main winding) is connected to the utility supply while the other winding set (auxiliary winding) is supplied by a PWM inverter as shown in Fig. 1. The voltage harmonics introduced by the inverter are filtered by the inherent inductances of the machine itself, and at sufficiently high PWM frequencies the approach should not require additional filtering. In addition, since the inverter requires only a single low-cost dc capacitor rather than three ac capacitors and switchgear is not needed to prevent overexcitation, this arrangement could eventually become a cost competitive alternative to more conventional methods of power factor correction of single machine units requiring on-site correction.

Manuscript received April 1, 1987; revised June 6, 1988. This paper was presented at the International Conference on the Evolution and Modern Aspects of Induction Machines, Turin, Italy, July 1986.

E. Muljadi is with the Department of Electrical Engineering, California State University, Fresno, CA 93740.

T. A. Lipo and D. W. Novotny are with the Department of Electrical and Computer Engineering, University of Wisconsin, Madison WI 53706.

IEEE Log Number 8931165.

PRINCIPLE OF OPERATION

When the PWM converter of Fig. 1 is instrumented with a suitable feedback control, the main winding of the induction machine can be controlled to carry only the active power while the flow of power in the auxiliary winding is solely the reactive component. Since the auxiliary winding carries only the reactive power, the PWM inverter dc voltage can be supported by a dc capacitor only and need not be connected to a power source. In effect the PWM inverter serves to act as a buffer to circulate reactive power between the machine windings and the dc capacitor. The PWM inverter can be controlled in such a manner so as to always provide the desired power factor at the terminals of the main winding. With sufficient ampere-turn capability of the auxiliary winding, unity power factor operation at the terminals of the main winding is possible over a wide range of load conditions including rated load. This paper sets forth the analysis of the steady-state characteristics of this power factor correction scheme as well as a discussion of the control algorithm required to realize this mode of operation.

EQUIVALENT CIRCUIT ANALYSIS

The principle of solid state excitation of an induction motor can be examined by means of the "per phase" equivalent circuit of Fig. 2, [7]. It can be noted that the rotor circuit and the main magnetic circuit are identical to that of a three-phase machine. The dual stator windings can be effectively modeled by two branches each having

0885-8993/89/1000-0409$01.00 © 1989 IEEE

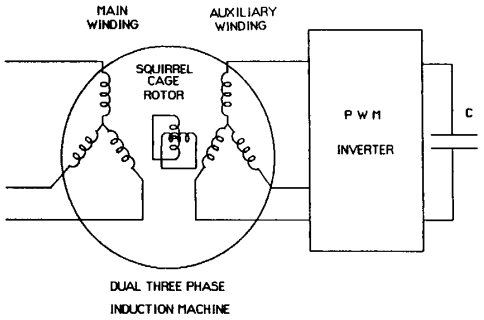

Fig. 1. Induction machine with auxiliary PWM inverter excitation.

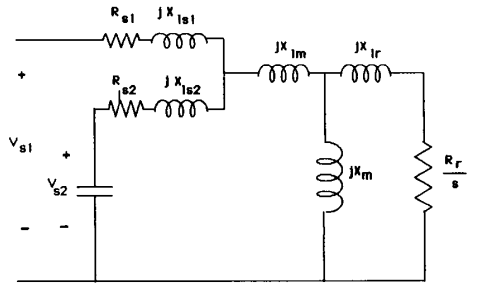

Fig. 2. Equivalent circuit of dual three-phase induction machine.

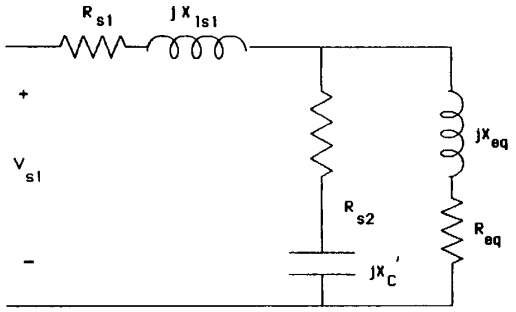

Fig. 3. Modified equivalent circuit.

separate resistance and leakage reactance together with a common mutual incidence X_{lm}, which occurs due the fact that the two sets stator windings occupy the same slots and are therefore mutually coupled by their leakage flux (i.e., non-air gap component of stator flux) [7]. When the PWM converter is controlled to pass only reactive power its effect can be represented in the equivalent circuit by a variable capacitor, which is functionally dependent on the voltage across and the current through the capacitor [8], [9].

To reduce the complexity of this analysis, it is useful to simplify the equivalent circuit to that of Fig. 3 wherein, for a fixed slip s,

$$X_c' = \frac{1}{\omega C} - X_{ls2} \tag{1}$$

$$X_{eq} = \text{Im}\left[jX_{lm} + \left(\frac{R_r}{s} + jX_{lr}\right)//jX_m\right] \tag{2}$$

$$R_{eq} = \text{Re}\left[\frac{R_r}{s} + jX_{lr}//jX_m\right] \tag{3}$$

where the "//" symbol indicates that the two impedances are in parallel. At a specific slip the circuit of Fig. 3 will operate at unity power factor when the imaginary part of the stator impedance viewed from the main winding becomes zero. The impedance of the rotor circuit in parallel with the auxiliary winding circuit can be written as

$$Z = \frac{(R_{s2}R_{eq} - X_c'X_{eq}) + j(X_c'R_{eq} + X_{eq}R_{s2})}{(R_{s2} + R_{eq}) + j(X_c' + X_{eq})}. \tag{4}$$

The imaginary part of the impedance is

$$\text{Im } Z = \frac{(X_c'R_{eq} + X_{eq}R_{s2})(R_{s2} + R_{eq}) - (R_{s2}R_{eq} - X_c'X_{eq})(X_c' + X_{eq})}{(R_{s2} + R_1)^2 + (X_c' + X_{eq})^2}. \tag{5}$$

Unity power factor requires that the imaginary part of the total input impedance of the induction machine equal zero, in which case

$$\text{Im } Z_{\text{tot}} = X_{ls1} + \text{Im } Z = 0 \tag{6}$$

or, hence

$$\text{Im } Z = -X_{ls1}. \tag{7}$$

Utilizing (7), (5) can be expressed as

$$a(X_c')^2 + bX_c' + c = 0 \tag{8}$$

where

$$a = X_{eq} + X_{ls1}$$

$$b = -R_{s2}R_{eq} + (R_{s2} + R_l)R_{eq} + 2X_{eq}X_{ls1}$$

$$c = -X_{eq}[R_{s2}R_{eq} - (R_{s2} + R_{eq})R_{s2}] + X_{ls1}[(R_{s2} + R_{eq})^2 + X_{eq}^2]$$

and a, b, c are constants at a specific speed.

Equation (8) is a simple quadratic equation that can be readily solved by the quadratic formula. A solution for X_c' clearly exists only if $b^2 - 4ac \geq 0$, which depends on the slip of the induction machine. Fig. 4 demonstrates how the imaginary part of Z_{tot} varies with X_c' for a typical machine having the parameters given in the Appendix. It can be noted that there are two values of X_c', which satisfies the condition of unity power factor for any specific slip. The smaller value of X_c' corresponds to a high current (large C), and the larger value of X_c' (smaller C) corresponds to a small value of current. Fig. 5 indicates how the locus of X_c' varies with slip for both a motoring and a generating condition.

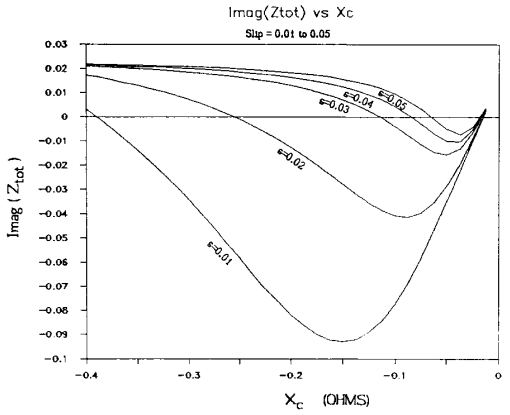

Fig. 4. Imaginary part of Z_{tot} versus X_c' for various values of slip.

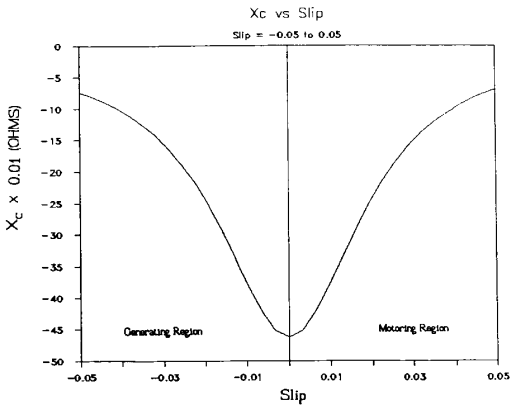

Fig. 5. Critical value of X_c' to produce unity power factor for motoring and generating conditions.

It can be seen from the equivalent circuit that with a fixed capacitor value the power factor varies with the slip. To illustrate this concept, it is useful to employ a current locus diagram. If the resistance and the leakage reactance of the main winding are neglected for simplicity and the stator mutual leakage is shorted ($X_{lm} \approx 0$) the simplified circuit diagram of Fig. 6 can be constructed. The admittance of the auxiliary winding branch can be written as

$$R_{s2} + jX_c' = \frac{1}{Y_{s2}} = \frac{1}{G_{s2} + jB_{s2}} \tag{9}$$

or

$$R_{s2} = \frac{G_{s2}}{G_{s2}^2 + B_{s2}^2} \tag{10}$$

so that

$$G_{s2}^2 - \frac{G_{s2}}{R_{s2}} + B_{s2}^2 = 0, \tag{11}$$

which can be written as

$$\left(G_{s2} - \frac{1}{2R_{s2}}\right)^2 + B_{s2}^2 = \left(\frac{1}{2R_{s2}}\right)^2. \tag{12}$$

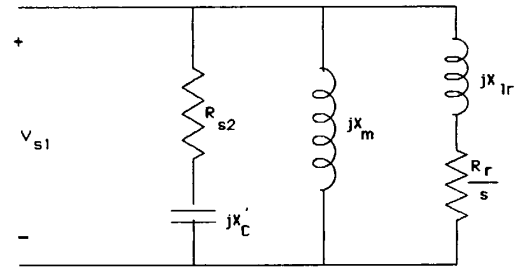

Fig. 6. Simplified equivalent circuit for modelling of current locus diagram.

Equation (12) is an expression for a circle on the $G - B$ plane, which has its center at $(1/2R_{s2}, 0)$ and for which the radius is $1/2R_{s2}$. The radius of the circle is inversely proportional to the size of the resistance R_{s2}.

Using the same approach, the equation for the rotor circuit can be represented as

$$G_r^2 + \left(B_r + \frac{1}{2X_{lr}}\right)^2 = \left(\frac{1}{2X_{lr}}\right)^2. \tag{13}$$

where, in this case $G_r + jB_r = Y_r$. This equation denotes a circle whose radius and center is dictated by the inverse of the rotor leakage reactance.

Consider now the admittance diagram for the entire circuit of Fig. 6. In Fig. 7 the total admittance Y_{tot} is found by adding the admittance of the auxiliary winding Y_{s2} to the admittance of the rotor Y_r and the magnetizing branch Y_m. The total admittance becomes

$$Y_{tot} = Y_{s2} + Y_r + Y_m.$$

The admittance Y_m serves to translate the admittance diagram down by $1/X_m$.

The corresponding current locus is given in Fig. 8 in which the fixed currents I_{s2} and I_m due to the admittances Y_{s2} and Y_m are added to various values of I_r. The vector sum of the three currents results in the main stator winding current. The sketch clearly shows why there exists two values of X_c' for which the total current is in phase with V_{s1}. While the equivalent circuit of Fig. 6 is an approximation, the general behavior of the detailed circuit, Fig. 2, remains the same. In practice the larger value of X_c' is chosen since this value not only corresponds to a smaller value of equivalent inverter capacitance but also to a smaller total current.

As slip of the machine varies, the semicircle locus of Y_{s2} effectively moves along the perimeter of the locus of Y_r. It can be observed that for both motoring and generating operation and for practical-sized capacitors there may exist a slip limit beyond which the induction machine will not operate at unity power factor. However, for most machines this limit will occur beyond the normal operating slip region. It is also evident that there is a possibility that there may not exist a value of X_c' that corresponds to unity power factor for a specific value of Y_r since R_{s2} affects the radius of the semicircle. From Fig. 8 the following conclusions can be obtained.

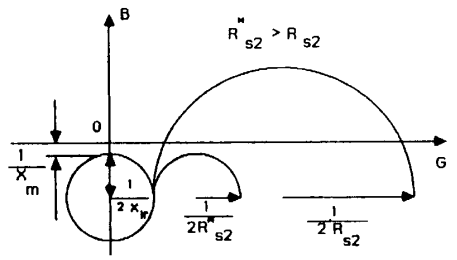

Fig. 7. Admittance diagram as function of X'_c for fixed value of slip and for two values of auxiliary winding resistance.

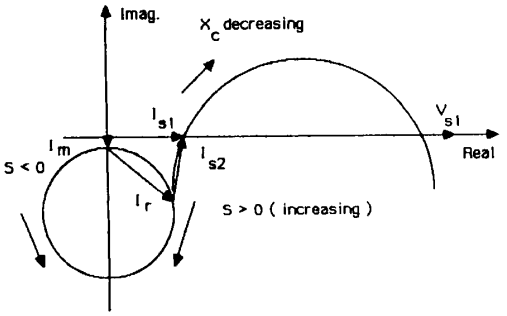

Fig. 8. Current locus diagram for fixed slip as function of x'_c. Unity power factor condition explicitly shown.

1) For a given induction machine there may be a limited range of slip for which a permissible value of X_c exists.

2) To enlarge the possibility of unity power factor for an induction machine the following parameters must be considered in the machine design.

(a) R_{s2} must be made as small as possible to maximize the circle diagram of the auxiliary branch.

(b) X_m must be made as large as possible to minimize the downward shift of the Y_{s2} and Y_r loci.

(c) X_{lr} must be made as small as possible to maximize size of the circle diagram of the rotor branch.

Steady-State Control Strategy

A phasor diagram of a dual three-phase induction machine can be readily constructed from the equivalent circuit of Fig. 2 and is shown in Fig. 9 for the unity power factor condition. In order to simplify the phasor analysis the equivalent circuit and resulting phasor diagram have been constructed by neglecting the leakage inductance in the main winding. This assumption is based on the fact that the leakage reactance will consume only a few percent of the total reactive power. The voltage $\tilde{V}_{s1}$ corresponds to the main winding stator voltage. At unity power factor the terminal voltage V_{s1} and the voltage V_{s12} are colinear and

$$V_{s12} = V_{s1} - I_{s1}R_{s1} \tag{14}$$

The current through the auxiliary winding will be

$$\tilde{I}_{s2} = \frac{\tilde{V}_{s12}}{R_{s2} + j(X_{ls2} - X_c)}. \tag{15}$$

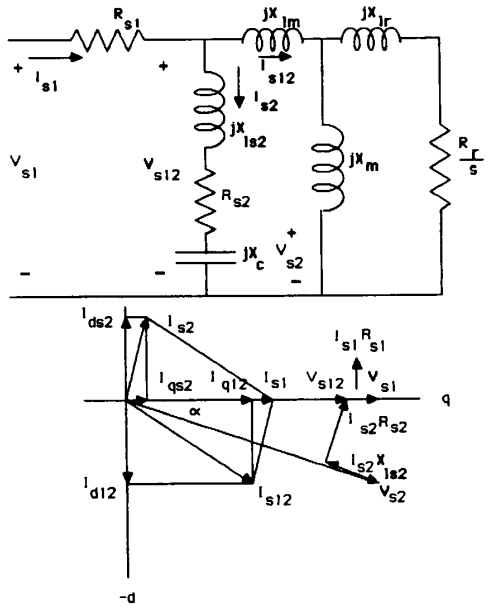

Fig. 9. Motor equivalent circuit and phasor diagram for main winding unity power factor operation.

Since R_{s2} is small the current $\tilde{I}_{s2}$ is almost perpendicular to $\tilde{V}_{s12}$. The total current into the magnetizing branch and the rotor circuit is

$$\tilde{I}_{s12} = \tilde{I}_{s1} - \tilde{I}_{s2} \tag{16}$$

In d-q notation this current can be written in terms of real variables as

$$I_{q12} = I_{qs1} - I_{qs2} \tag{17}$$

and

$$I_{d12} = -I_{ds2}. \tag{18}$$

The voltage output of the PWM is

$$\tilde{V}_{s2} = \tilde{I}_{s2}(-j)X_c \tag{19}$$

$$= (\tilde{I}_{qs2} + j\tilde{I}_{ds2})(-jX_c) \tag{20}$$

or

$$V_{qs2} = I_{ds2}X_c \tag{21}$$

and

$$V_{ds2} = -I_{qs2}X_c. \tag{22}$$

The reactive power consumed by the rotor and magnetizing branch of the machine can be written as

$$Q_{s12} = V_{q12}I_{d12} + V_{d12}I_{q12}. \tag{23}$$

The reactive power produced by the PWM can be written as

$$Q_{s2} = V_{s2}I_{s2}. \tag{24}$$

Equation (24) can also be written in d-q as

$$Q_{s2} = V_{qs2}I_{ds2} + V_{ds2}I_{qs2}. \tag{25}$$

The active power needed to compensate the losses in the auxiliary winding is

$$P_{s2} = V_{s12} I_{s2} \sin \alpha \tag{26}$$

where α denotes the angle between the phasors V_{s1} and V_{s2}. In terms of d-q variables

$$P_{s2} = V_{q12} I_{qs2}. \tag{27}$$

The control strategy for tentative controller can be arranged according to these equations. However, the variable to be controlled in the real circuit is different from the equivalent circuit, Fig. 2. In the equivalent circuit it is assumed there is a variable capacitor that can be controlled as desired. The variable in the actual system is the magnitude and phase of the PWM inverter and the sensed variables are the reactive power input to the main winding and the dc voltage across the dc bus. It is useful to demonstrate how the controlled variables (PWM inverter voltage amplitude and phase) affect the regulation of the sensed feedback signals (main winding power factor and dc inverter voltage).

In a conventional induction machine the stator current normally lags the stator voltage. The function of the PWM is to inject a reactive current I_{s2} into the machine so that the resultant of the two currents will be in phase with the voltage supply V_{s1}. Since the PWM used is a voltage source inverter, the only means to modulate the current I_{s2} is by modulating the voltage V_{s2} (output voltage of the PWM). The reactive power of the main winding is used to modulate the magnitude of V_{s2} or I_{s2} indirectly. The reactive power demanded by the induction machine is approximately

$$Q \approx -V_{q12} I_{d12} = V_{q12} I_{ds2}. \tag{28}$$

From the phasor diagram it can be seen that the angle α is small, which makes V_{ds2} and I_{qs2} small, so the product of the two $V_{ds2} I_{qs2}$ can be neglected. Therefore, from (25), the reactive power produced by the PWM can be written as

$$Q_{s2} \approx V_{qs2} I_{ds2}. \tag{29}$$

To increase the reactive power produced by the PWM circuits, the real component of auxiliary winding voltage V_{qs2} can be increased. In the equivalent circuit this means the size of effective capacitive reactance X_c must be increased. In the actual circuit this can be accomplished by adjusting the pulsewidth of the PWM. Since the angle α is always small, then

$$I_{ds2} \approx I_{s2}. \tag{30}$$

This result demonstrates that by adjusting the magnitude of V_{s2}, the magnitude of the reactive power produced by the PWM can be adjusted accordingly.

Another variable that can be controlled is the phase angle of the PWM output voltage. This angle is related to the active power flow between induction machine and PWM. From (26) it can be seen that if the angle α is not correctly adjusted there will be an interchange of active power between the main power and PWM. Assume, for example, that the angle α is too large. In this case the active power entering the auxiliary winding from the main winding is not only used to compensate the losses in R_{s2} but also to charge the dc capacitor. As a result, the dc voltage will increase due to charging current into the capacitor. On the other hand, if the angle α is too small there will be a discharging current out of the capacitor that will reduce the dc voltage. The angle α of the PWM output voltage is therefore most convenient for use as a control variable to regulate the dc inverter voltage.

It is clear that the auxiliary winding must carry the reactive ower required by the induction machine. Net active power is required by the auxiliary winding to compensate the copper losses $I_{s2}^2 R_{s2}$. This small portion of active power is transferred from the main winding to the auxiliary winding. Thus the active power due to the losses in the auxiliary winding must be considered in the design of the winding.

Fig. 10 illustrates how the auxiliary winding voltage amplitude and phase angle with respect to the main winding voltage must be varied with slip (i.e., load) to preserve unity power factor at the main winding terminals and keep the inverter dc voltage constant. It is clear that the relatively small variations in V_{s2} and α are required over a wide change in load suggesting that tight control of the PWM inverter output voltage will be required for satisfactory operation.

The per unit value of the fundamental component of the auxiliary voltage will be approximately the same as the main voltage supply since the voltage drop across the impedance of the stator (main and auxiliary winding) is relatively small. However, the dc voltage must be sufficiently high so that the PWM can be modulated with a suitable chopping frequency to yield a smooth current waveform on the main winding. As can be seen from Figs. 7 and 8, as the slip increases, the reactive power and thus I_{s2} also increases. Consequently the copper losses in the auxiliary winding also increases. From Fig. 10 it is shown that α increases with the slip suggesting that there is an increase in active power flow from the main winding into the auxiliary winding. Depending on the design of the auxiliary winding, if the resistance R_{s2} of the auxiliary winding can be made small, the angle α variation will also be small.

The VA rating of the PWM can be estimated to have the same var requirement (reactive power) as normally needed by the induction machine without an auxiliary winding. The voltage (fundamental component) rating will be approximately equal to the main supply voltage and the current rating must be rated at the reactive part of the total current normally required by the induction machine. It should be noted that the dc bus voltage must be designed to enable the PWM (at a high chopping frequency) to generate an output voltage with fundamental component approximately equal to or greater than the main supply voltage.

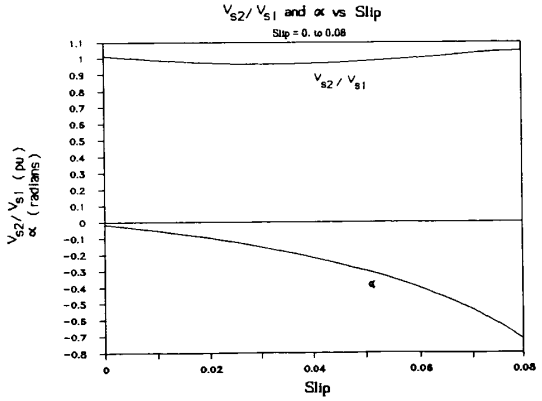

Fig. 10. Per unit inverter amplitude V_{s2}/V_{s1} and phase angle α required to maintain zero main winding reactive power and constant dc-inverter voltage as function of slip.

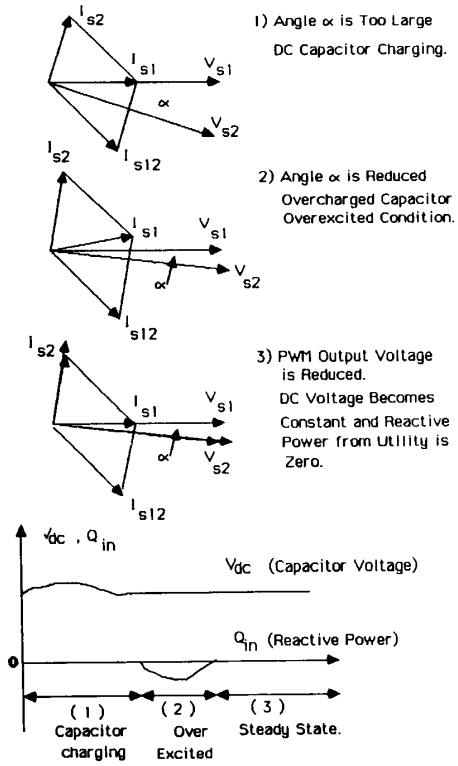

Fig. 11. Illustration of control philosophy utilizing inverter amplitude and phase angle control.

The use of voltage amplitude and phase angle control (α control) to simultaneously adjust the main winding reactive power and capacitor voltage is illustrated in Fig. 11. In Step 1) it is assumed that the control angle α is too large so power flows into the inverter thereby charging the dc side capacitor. In order to prevent further charging the overvoltage condition is sensed and α decreased until the capacitor voltage becomes constant. Regardless of the value of dc voltage obtained, the reactive power to the main winding can now be regulated to zero by maintaining a constant α angle and adjusting the amplitude of the inverter output ac voltage by pulsewidth modulation. In practice the control of dc voltage and main winding reactive power control occurs simultaneously and the dc voltage is continuously regulated to a desired nominal value.

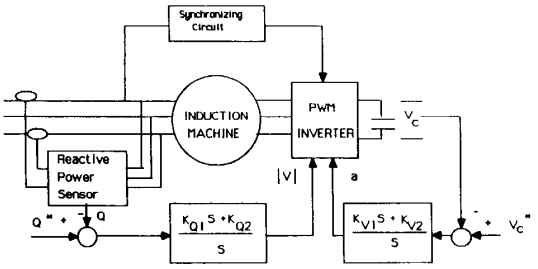

Fig. 12. Control block diagram of overall system.

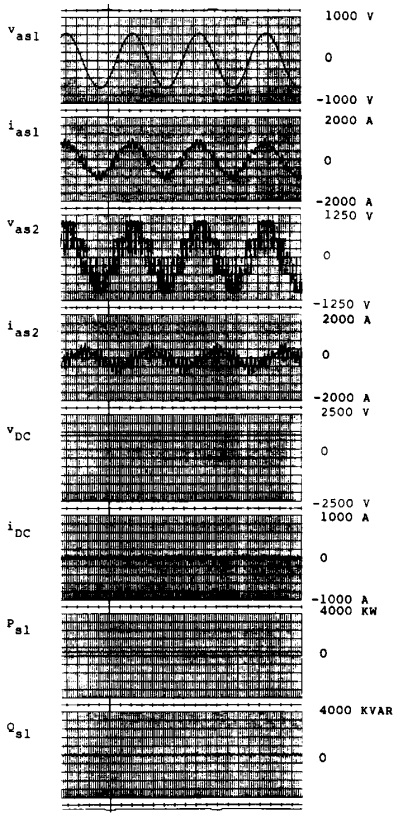

Fig. 13. Analog simulation result for unity power factor operation of main winding using PWM inverter with 12 chops/cycle (600 Hz), $C = 70\,000$ μF. Explanation of symbols; applicable to Figs. 13–16: v_{as1}, i_{as} – main winding phase to neutral voltage and line current. v_{as2}, i_{as2} – auxiliary winding phase to neutral voltage and line current. v_{DC}, i_{DC} – inverter dc voltage and current. P_{s1}, Q_{s1} – main winding power and reactive power.

Analog Computer Simulation Results

In order to demonstrate the feasibility of the approach an analog simulation of the entire system has been carried out including detailed simulations of the dual three-phase induction machine, the vertical speed indicator (VSI)–PWM inverter and controller. The overall block diagram of the entire system is shown in Fig. 12. The induction motor wound for dual three-phase operation in the simulation was rated at 920 hp, 460 V, six poles, 50 Hz, 5/6

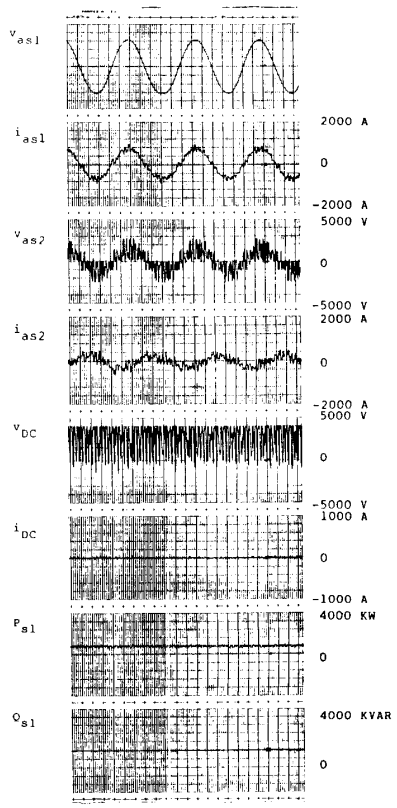

Fig. 14. Analog computer result for main winding unity power factor operation using PWM inverter with 12 chops/cycle, $C = 700$ μF.

pitch. Parameters of the motor used are as follows:

R_{s1} 0.0070 Ω
X_{ls1} 0.00728 Ω
X_{ls2} 0.00728 Ω
X_m 0.4620 Ω
R_r 0.00204 Ω
X_{lr} 0.00697 Ω.

The main winding is connected to the utility supply while the auxiliary winding is supplied by the PWM inverter. The PWM inverter is operated at constant frequency (same as main supply frequency) and at a constant PWM modulation frequency. Only a dc capacitor is connected to the dc side of the inverter. The pulsewidth is used to vary the magnitude of the inverter output voltage and therefore regulate the reactive power supplied by the main winding. The phase shift between the fundamental component of the resulting output voltage with respect to the main supply voltage is used to regulate the capacitor voltage (inverter dc voltage).

The analog traces of Figs. 13–16 summarize the results of a computer study that was conducted to verify the validity of the approach and to establish how the PWM switching frequency and inverter dc capacitance affect behavior of the system. It can be noted that the dc voltage (capacitor voltage) is very smooth. Operation of the sys-

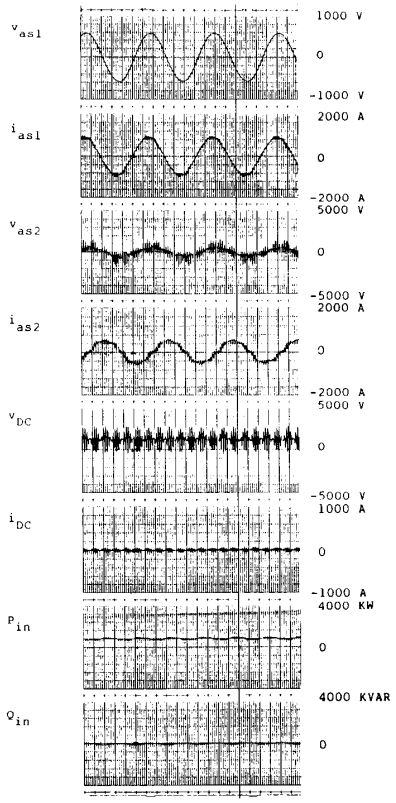

Fig. 15. Simulation result utilizing a PWM inverter with 30 Chops/Cycle, (1500 Hz), $C = 2000\ \mu F$.

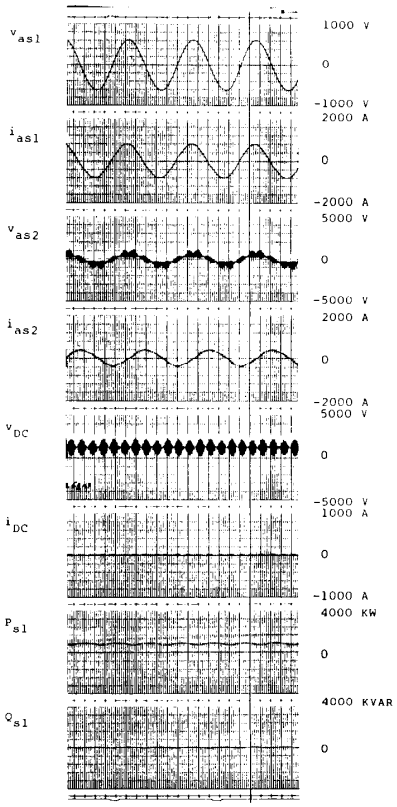

Fig. 16. Analog trace for main winding unity power factor operation with PWM inverter having 60 chops/cycle (3000 Hz), $C = 2000\ \mu F$.

tem with a relatively large dc capacitor value of 70 000 μF but a low chopping frequency of 600 Hz is shown in Fig. 13. It is interesting to note that the harmonic current of the main winding current is significantly less than the auxiliary winding current. It appears that while filtering action is being provided by the series leakage inductance existing between the main and auxiliary windings, substantial filtering is also derived from the rotor circuit, which is effectively in parallel with the auxiliary winding impedance. In effect the rotor of the machine acts as a "zero-cost rotating filter."

For the simulation study reported in this paper the machine selected was assumed to have equal ampere turns in the main and auxiliary windings and that the windings were placed in the slots in symmetrical fashion [8]. However, the coupling between the auxiliary winding and the rotor bars can be enhanced by winding the machine so that the auxiliary winding is on the surface of the slot nearest the air gap. The filtering action of the rotating rotor bars is a new concept that has attracted little attention. Work on design of a special purpose machine is continuing and will be reported in a future paper.

For comparison with Fig. 13, the capacitor value has been reduced to only 700 μF in Fig. 14. It can be noted that the ripple on the dc voltage has increased considerably. However, the ripple in the input current to the main winding has actually decreased somewhat again suggesting the effectiveness of the rotating filter in removing unwanted harmonics from the main winding current.

The effect of changes in the PWM frequency can be seen by comparing analog traces, Figs. 15 and 16. In this case the dc capacitor has been fixed at 2000 μF. The PWM frequency is 1500 Hz for Fig. 15 and 3000 Hz for Fig. 16. It can be noted that the higher modulating frequencies result in a much less distorted main winding current. If the PWM chopping frequency can be raised to approximately 3000 Hz the ripple current in the main winding becomes completely negligible. It is also clear from Figs. 15 and 16 that for the same size of the ripple dc voltage, a higher modulating frequency permits the use of a smaller capacitor.

Fig. 17 illustrates the transient behavior of the power factor controller. In particular, the reactive power command Q^* is suddenly changed to a positive value (i.e., leading power factor at the main winding). At time t_1 the commanded value of reactive power is again reduced to zero. It can be noted that the response to the changes requires only several cycles and is well damped. The average value of the inverter dc voltage is essentially unaffected during the transient.

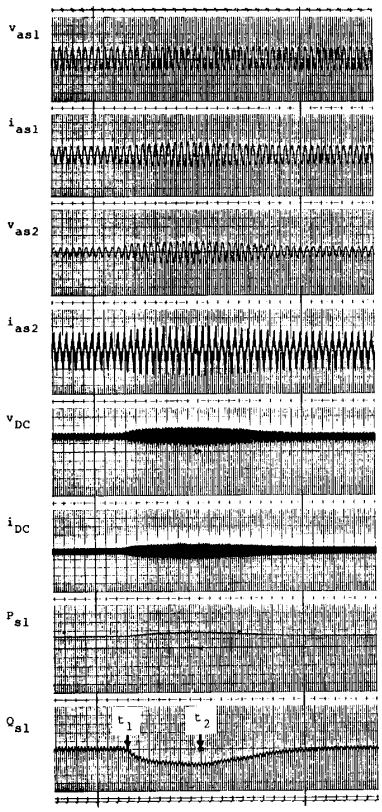

Fig. 17. Simulation results showing transient response of power factor controller. At time t_1 reactive power command is increased to positive value (leading power factor). At t_2 command is reduced to zero.

Conclusion

This paper has reported preliminary results of a new approach to self-excitation of an induction machine. In this approach the machine is equipped with an extra three-phase winding to specifically carry the reactive power required by the machine. The main winding of the machine is connected to the utility and is thus able to operate at unity or even leading power factor in much the same manner as a synchronous machine. The excitation power supplied to the extra auxiliary winding is derived from a PWM inverter operating with a floating dc capacitor. Thus the ac/dc converter normally associated with power flow on the dc side of the inverter is not required. Simulation results indicate that with PWM frequencies of sufficiently large value will permit application without the need for additional filtering of the motor current seen by the utility supply.

While the work reported in this paper relates specifically to an induction motor, the principle is readily extended to an induction generator. In particular, this new concept of excitation should prove very useful for excitation of induction machines in isolated systems supplying passive r–L loads. A study of this mode of operation is underway at the University of Wisconsin.

References

[1] H. Achenbach, W. Hanke, and W. Hochstetter, "Controllable static power compensators in electric supply system," in Proc. IFAC, 1977, p. 917.

[2] L. Gyugyi and E. C. Strycula, "Active ac power filters," *in Proc.* 1976, p. 529, IEEE/IAS Annual Meeting.

[3] P. M. Espelage and B. K. Bose, "High-Frequency Link Power Conversion," *IEEE Trans. Ind. Appl.*, vol. IA-13, p. 387-394, 1977.

[4] L. Gyugyi, "Reactive power generation and control by thyristor circuits," *IEEE Trans. Ind. Appl.*, vol. IA-15, no. 5, pp. 521-531, 1979.

[5] I. Takahashi and A. Nabae, "Universal power distortion compensator of line commutated thyristor converter," in *Proc. IEEE/IAS Annual Meeting*, p. 858-864, 1980.

[6] Y. Harumoto, Y. Hasegawa, T. Yano, M. Ikeda, and K. Matsuura, "New static VAR control using force-commutated inverters," presented at *IEEE/PES Winter Meeting*, 1981.

[7] T. A. Lipo, "A d-q model for six phase induction machines," *International Conference on Electrical Machines*, Sept. 15-17, 1980, Athens, Greece, pp. 860-867.

[8] P. C. Krause and T. A. Lipo, "Analysis and simplified representations of rectifier-inverter reluctance-synchronous motor drives," *IEEE Trans. Power App. Syst.*, vol. PAS-88, no. 6, pp. 962-970, June 1969.

[9] J. A. A. Melkebeek and D. W Novotny, "Steady state modelling of regeneration and self-excitation in induction machines," *IEEE Trans. Power App. Syst.*, vol. PAS-102, pp. 2725-2733, Aug. 1983.

Eduard Muljadi (S'83-S'84-M'84-M'87) was born in Surabaya, Indonesia, on November 27, 1957. He received the E.E. degree from Surabaya Institute of Technology, Surabaya, Indonesia, in 1981, and the M.S.E.E. and Ph.D. degrees from the University of Wisconsin-Madison, in 1984 and 1987, respectively.

Since 1988 he has been a Faculty Member of the Department of Electrical Engineering at California State University, Fresno, CA.

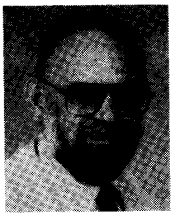

Thomas A. Lipo (M'64-SM'71-F'87) received the B.E.E. and M.S.E.E. degrees from Marquette University, Milwaukee, WI, and the Ph.D. degree in electrical engineering from the University of Wisconsin-Madison, in 1962, 1964, and 1968, respectively.

From 1969 to 1979 he was an Electrical Engineer in the Power Electronics Laboratory of Corporate Research and Development of the General Electric Company, Schenectady, NY. In 1979 he became Professor of Electrical Engineering at Purdue University, Lafayette, IN. He joined the faculty of the University of Wisconsin in 1981, where he is presently a Professor of Electrical Engineering. He has maintained a deep interest in power electronics and ac drives for over 25 years.

Dr. Lipo holds 10 patents, has published over 100 papers and has received 11 prize paper awards. He is an active member of five IEEE Committees or Subcommittees and is past Chairman of two of them. He is also a member of the Executive Board of the Industry Applications Society and Editor of the IEEE TRANSACTIONS ON POWER ELECTRONICS.

Donald W. Novotny (M'80–F'87) received the B.S. and M.S. degrees in electrical engineering from the Illinois Institute of Technology, Chicago, in 1956 and 1957, respectively, and the Ph.D. degree from the University of Wisconsin–Madison in 1961.

Since 1961 he has been a member of the faculty of the University of Wisconsin–Madison, where he is currently Professor and Co-Director of the Wisconsin Electric Machines and Power Electronics Consortium (WEMPEC). He served as Chairman of the Electrical and Computer Engineering Department from 1976 to 1980 and as an Associate Director of the University-Industry Research Program from 1972 to 1974 and from 1980 to the present. He has been active as a consultant to many organizations and a Visiting Professor at Montana State University, Bozeman, MT, the Technical University of Eindhoven, Eindhoven, Netherlands, the Catholic University of Leuven, Leuven, Belgium, and a Fulbright Lecturer at the University of Ghent, Ghent, Belgium. His teaching and research interests include electric machines, variable frequency drive systems, and power electronic control of industrial systems.

Dr. Novotny is a member ASEE, Sigma Xi, Eta Kappa Nu, and Tau Beta Pi, and is a Registered Professional Engineer in the State of Wisconsin.